Alexandria Engineering Journal (2014) 53, 399–408

Alexandria University

Alexandria Engineering Journal

www.elsevier.com/locate/aej
www.sciencedirect.com

ORIGINAL ARTICLE

Adsorptive removal of nickel from aqueous solutions by activated carbons from doum seed (*Hyphaenethebaica*) coat

Manal El-Sadaawy, Ola Abdelwahab *

Environmental Division, National Institute of Oceanography and Fisheries, Kayet Bay, El-Anfushy, Alexandria, Egypt

Received 7 February 2014; revised 20 March 2014; accepted 27 March 2014
Available online 5 May 2014

KEYWORDS

Adsorption;
Nickel (II);
Activated carbon;
Equilibrium isotherm;
Error analysis

Abstract The present study investigates the possibility of using low cost agriculture waste as doum-palm seed coat for the removal of nickel ions from aqueous solutions. Two activated carbons had been prepared from raw doum-palm seed coat (DACI and DACII); as well, the raw material was used as an adsorbent (RD). Batch adsorption experiments were performed as a function of pH of solution, initial nickel ions concentration, dose of adsorbent and contact time. Adsorption data were modeled using Langmuir, Freundlich, Temkin and D–R Models. Different error analysis conforms that the isotherm data followed Freundlich models for all adsorbents. Adsorption kinetic data were tested using pseudo-first order, pseudo-second order and Elovich model. Adsorption mechanism was investigated using the intra-particle diffusion model. Diffusion coefficients were calculated using the film and intraparticle diffusion models. Kinetic studies showed that the adsorption of Ni^{2+} ions onto RD, DACI and DACII followed pseudo-second order kinetic model, and indicates that the intra-particle diffusion controls the rate of adsorption but it is not the rate limiting step.

1. Introduction

The pollution of heavy metals has gained worldwide attention due to their toxicity, difficult degradation, and accumulation in the living organisms. Therefore, treatment of wastewater contaminated by heavy metals is an important environmental concern [1]. Nickel was selected as an adsorbate because its compounds have widespread applications in many industrial processes such as non-ferrous metal, mineral processing, paint formulation, electroplating, batteries manufacturing, porcelain enameling, copper sulfate manufacture and steam-electric power plants leading to relatively high concentrations in aquatic environment [2]. Some nickel compounds, such as nickel carbonyl, are carcinogenic and easily absorbed by the skin. The exposure to this compound, at an atmospheric concentration of 30 mg/l for half an hour, is lethal [3]. High concentration of nickel causes cancer of lungs, nose and bone [4,5]. At

* Corresponding author. Tel.: +20 1221093161; fax: +20 3 4801553.
E-mail address: olaabdelwahab53@hotmail.com (O. Abdelwahab).

Peer review under responsibility of Faculty of Engineering, Alexandria University.

ELSEVIER Production and hosting by Elsevier

1110-0168 © 2014 Production and hosting by Elsevier B.V. on behalf of Faculty of Engineering, Alexandria University.
http://dx.doi.org/10.1016/j.aej.2014.03.014

very high levels of exposure, nickel salts are known to be carcinogenic [2]. Consequently, there is a need to treat industrial effluents polluted with Ni^{2+} ions before their discharge into the receiving water bodies. The US EPA has set specific nickel limits for wastewater effluent which are 2 mg/l for short-term effluent reuse and 0.2 mg/l for long-term effluent reuse [6].

Many conventional methods including oxidation, membrane filtration, coagulation, reverse osmosis, adsorption, ion exchange, precipitation have been reported in the literature to remove heavy metals from waste water. These methods may be ineffective or extremely expensive especially when the waste stream contains relatively low concentration of metal (1–100 mg/l) dissolved in large volume [7]. However, adsorption can be regarded as one of the most popular methods for the removal of heavy metals from the wastewater due to its low cost, easy availability, biodegradability, simplicity of design and high removal efficiency [8]. Activated carbon has been found the most promising and widely used adsorbent in wastewater pollution control throughout the world and has been successfully utilized for the removal of diverse types of pollutants including metal ions. However, the high capital and regeneration cost of activated carbon limits its large scale applications for the removal of metals and other aquatic pollutants, which has encouraged researchers to look for low-cost alternative adsorbents. The utilization of agro-wastes as adsorbent is currently receiving wide attention because of their abundant availability and low-cost owing to relatively high fixed carbon content and presence of porous structure [2].

The present study aims to investigate the adsorption of Ni^{2+} ions from aqueous solutions onto activated carbon prepared from a low cost agricultural by product such as doum palm seed. The effect of initial metal ion concentration was studied and the relationship between pH and removal efficiency was also analyzed. The Langmuir, Freundlich, Temkin and The Dubinin–Radushkevich models were utilized for analysis of the adsorption equilibrium. Kinetic models were tested to identify the potential adsorption process mechanisms. FTIR study was carried out to understand surface properties and available functional groups involved in sorption mechanism.

2. Materials and methods

2.1. Chemicals

All reagents were of AR grade chemicals. A stock solution of nickel (1000 mg/l) was prepared in double distilled water using nickel nitrate. All other solutions were prepared by diluting stock solution. The pH of the solution was adjusted with NaOH or HCl solutions and measured by pH meter (Model 744, metrohm). Nickel ions concentrations were determined with an atomic absorption spectrophotometer (Perkin Elmer 2380).

2.2. Preparation of adsorbent

Doum palm, *Hyphaene thebaica* L. (Palmae), is growing wild throughout the dry regions of tropical Africa, the Middle East and Western India [9]. The doum seed-coats were collected locally from Upper Egypt. They were first freed of the doum kernels by filling. Then, they were washed with distilled water and dried in an oven at 105 °C for 2 h. The dried seed coats were crushed and sieved to a suitable particle size. Activated carbons have been prepared from the above material using the method as described by Amin and Abdelwahab [10], i.e., by application of pyrolysis activation, and by application of chemical followed by physical activation. Part of crushed row doum seed coats was used as adsorbent termed (RD), while the other parts of the raw materials were subjected to two types of activation (i) physical activation by carbonization in a muffle furnace at 300 °C for 1 h, the absorbent obtained after carbonization is termed as DACI, (ii) Chemical treatment followed By soaking in 28% H_3PO_4 for 24 h, and then it was filtered and carbonized in the absence of air at 300 °C in a muffle furnace for 1 h, the absorbent obtained after carbonization is termed as DACII.

2.3. Adsorption isotherm

Batch adsorption experiments were carried out in a 250 ml stopper conical flask by adding 0.1–1.0 g of adsorbent and 100 ml of nickel nitrate solution of specific concentration. The concentration of Ni^{2+} solution was varied from 10 to 40 mg/l. All experiments were done at room temperature. The samples were shaken in a mechanical shaker for a contact time ranging from 5 to 180 min. The pH of the solutions was ranged from 1 to 7. After each experiment, the contents were filtered through a filter paper neglecting the first 5 ml of the filtrate in order to saturate the filter paper with nickel nitrate solution. Concentrations of nickel ions in the filtrate were then determined by atomic absorption spectrophotometer.

The amount of nickel adsorbed using the three adsorbents (RD, DACI and DACII) at equilibrium, q_e (mg/g), was calculated by the following mass balance relationship

$$\mathbf{q_e} = (\mathbf{C_0} - \mathbf{C_e}) \times \frac{\mathbf{v}}{\mathbf{w}} \quad (1)$$

where C_0 and C_e are the initial and equilibrium liquid-phase concentrations of nickel, respectively (mg/l), V the volume of the solution (l), and W is the weight of the adsorbate used (g).

3. Results and discussion

3.1. The effect of pH

The pH of the aqueous solution is an important parameter for the adsorption of both anions and cations at the liquid–solid interface. The binding of metal ions with surface functional groups was strongly pH dependent [11]. To determine the influence of pH, experiments were performed at various initial pH, ranging between 2 and 7. It is evidence from Fig. 1 that maximum adsorption of Ni^{2+} was (40.68%, 49.15% and 50.68%) for (Raw, DACI and DACII respectively) at pH 7.0. The pH dependency is both related to the surface properties of the activated carbon and nickel species in solution [12]. At low pH values, metal cations and protons compete for binding sites on adsorbent surface which results in lower uptake of metal. It has been suggested that at highly acidic condition, adsorbent surface ligands would be closely associated with H_3O^+ that restricts access to ligands by metal ions as a result of repulsive forces [13]. It is to be expected that with the increase in pH values, more and more ligands having negative charge would be exposed which result in increase in

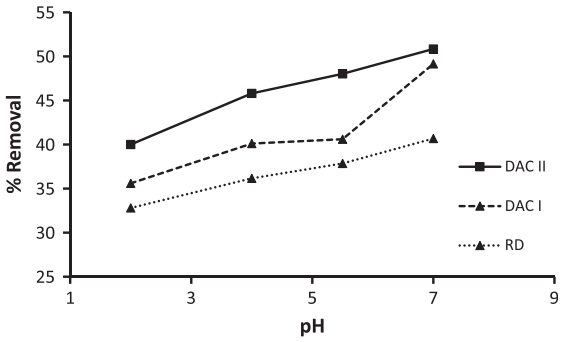

Figure 1 Effect of initial pH on the removal of Ni^{2+} ions using different adsorbents (dose of adsorbent: 5 g/l, concentration of Ni^{++} solution: 20 mg/l, time of agitation: 2 h).

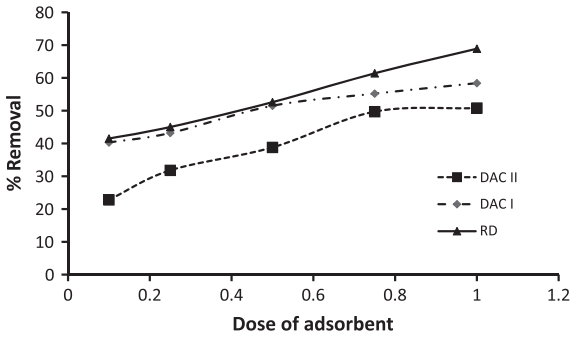

Figure 3 Effect of adsorbent dose on Ni^{++} percentage removal [solution pH:7, initial concentration of Ni^{2+} solution: 20 mg/l, contact time 2 h].

attraction of positively charged metal ions [14]. In addition, at higher pH, more than 7, the lower binding is attributed to reduced solubility of the metal and its precipitation [13].

3.2. Effect of initial concentration

The initial concentration of metal ion provides an important driving force to overcome all mass transfer resistances of metal ions between the aqueous and solid phases [15]. The sorption of Ni^{2+} ions onto various adsorbents was carried out at different initial Ni^{2+} ion concentrations ranging from 10 to 40 mg/l, at pH 7. Fig. 2 clearly shows that by increasing the concentration gradually there is a decrease in the percentage removal. As the ratio of sportive surface to ion concentration decreased with increasing metal ion concentration and so metal ion removal was reduced. At low initial concentration of metal ions, more binding sites are available. But as the concentration increases, the number of ions competing for available binding sites in the biomass increased [16].

3.3. Effect of adsorbent dose

Adsorption assays using different masses of adsorbent to adsorbate solution were carried out in order to assess the effect of adsorbent amount on Ni^{2+} removal. It is obvious from Fig. 3 that an increase in the removal percentage is noted as the amount of adsorbent used increases for RD, DACI and DACII, respectively. That is expected because at a fixed initial concentration of sorbate the increase in the adsorbent amount provides a larger surface area or adsorptive sites [17]. The decrease in adsorbed amount per unit mass of adsorbent is a generally observed behavior which is also reported by the many researchers [18–20]. This may be attributed to two reasons: (i) a large adsorbent amount effectively reduces the unsaturation of the adsorption sites and correspondingly, the number of such sites per unit mass comes down resulting in comparatively less adsorption at higher adsorbent amount, and (ii) higher adsorbent amount creates particle aggregation, resulting in a decrease in the total surface area and an increase in diffusional path length both of which contribute to decrease in amount adsorbed per unit mass [21].

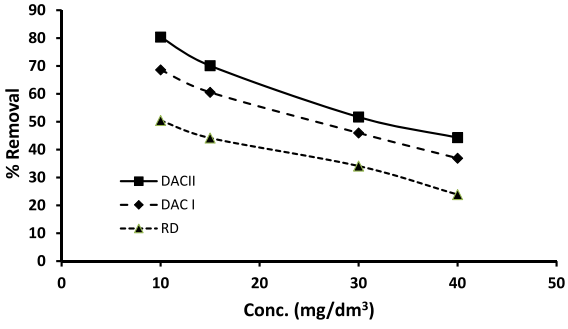

Figure 2 Adsorption of Ni^{2+} as a function of initial nickel concentration for different adsorbents [contact time: 2 h, adsorbent dose: 5 g/l and pH 7].

3.4. Adsorption isotherms

3.4.1. Adsorption isotherm models

Analysis of the equilibrium data is important to develop an equation which accurately represents the results and can be used for the design purposes [22]. Several isotherm equations have been used for the equilibrium modeling of adsorption systems. The sorption data have been subjected to different sorption isotherms, namely; Langmuir, Freundlich, Dubinin–Radushkevich (D–R) and Temkin. An adsorption isotherm is characterized by certain constants which values express the surface properties and affinity of the sorbent and can also be used to find the capacity of different sorbents. Based on ideal assumption of a monolayer, adsorption of adsorbate on adsorbent surface the Langmuir isotherm model [23] is expressed in linear form as follows:

$$\frac{1}{q_e} = \left(\frac{1}{K_l Q_m}\right)\frac{1}{C_e} + \frac{1}{Q_m} \tag{2}$$

where Q_m is the maximum monolayer adsorption capacity (mg/g) and K_l is the Langmuir constant which is related to the heat of adsorption (l/ mg). The values of Langmuir constants are presented in Table 1. The essential features of the Langmuir isotherm can be expressed in terms of dimensionless separation factor (R_L) given by [24]:

$$R_L = \frac{1}{(1 + K_l C_0)} \tag{3}$$

The value of separation factor R_L indicates either the adsorption isotherm to be unfavorable ($R_L > 1$), favorable ($0 < R_L > 1$), linear ($R_L = 1$) or irreversible ($R_L = 0$). The

Table 1 Isotherm constants for Ni^{2+} adsorption onto RD, DACI and DACII.

Isotherm model	Type of adsorbent		
	RD	DACI	DACII
Langmuir			
Q_m (mg/g)	3.24	4.93	13.51
K_l (l/mg)	0.28	0.289	0.296
R^2	0.776	0.947	0.896
Frundlich			
K_F (l/g)	0.98	0.8	0.36
n_F	2.39	2.27	1.75
R^2	0.992	0.986	0.896
Tempkin			
B_T (l/g)	2790	2878	3164
A (mg/l)	0.157	0.145	0.272
b_T	77.79	101.88	195.66
R^2	0.959	0.953	0.975
D–R			
q_m	2.78	3.64	11.93
E	0.03	0.022	0.02
R^2	0.724	0.753	0.839

values of separation factor R_L at different conditions were found to be in the range between 0 and 1, indicating the favorable adsorption of Ni^{2+} on RD, DACI and DACII, respectively.

The Freundlich sorption isotherm [25], one of the most widely used mathematical descriptions, usually fits the experimental data over a wide range of concentrations. This isotherm gives an expression encompassing the surface heterogeneity and the exponential distribution of active sites and their energies. The Freundlich adsorption isotherms were also applied to the removal of Ni^{2+} on RD, DACI and DACII.

$$\ln q_e = \ln K_F + \frac{1}{n_F} \ln C_e \tag{4}$$

where K_F and $1/n_F$ are the Freundlich constants. The values of K_F and n_F were calculated from the slope and intercept of the linear plot ln q_e versus ln C_e and reported in Table 1. The values of $n_F > 1$, reflecting the favorable adsorption conditions [26].

The Temkin isotherm equation assumes that the fall in the heat of adsorption of all the molecules in the layer decreases linearly with coverage due to adsorbent–adsorbate interactions, and that the adsorption is characterized by a uniform distribution of the binding energies up to some maximum binding energy [27]. The Temkin isotherm has been applied in the following form:

$$q_e = B_T \ln A + B_T \ln C_e \tag{5}$$

where $B_T = (RT)/b_T$, T is the absolute temperature in Kelvin and R is the universal gas constant (8.314 J/mol K). The model constants B_T and A are determined by the linear plot of q_e versus ln C_e. The Temkin isotherm assumes that the heat of adsorption of the molecules in a layer decreases linearly due to adsorbent–adsorbate interaction and that the binding energies are uniformly distributed [28]. Temkin constants are presented in Table 1.

The Dubinin–Radushkevich (D–R) model is given by [29]:

$$\ln q_e = \ln q_m - K_D \varepsilon^2 \tag{6}$$

$$\varepsilon = RT \ln\left(1 + \frac{1}{C_e}\right) \tag{7}$$

where q_m is the maximum sorption capacity of the adsorbent (mg/g), ε is the Polanyi sorption potential and K_D (mol^2/J^2) is a constant related to the mean energy of sorption per mole of adsorbate as it is transferred from the bulk solution to the surface of the solid. This energy E is determined by the following equation [30]:

$$E = \frac{1}{\sqrt{(2K_D)}} \tag{8}$$

It is known that magnitude of apparent adsorption energy E is useful for estimating the type of adsorption and if this value is below 8 kJ/mol the adsorption type can be explained by physical adsorption, between 8 and 16 kJ/mol the adsorption type can be explained by ion exchange, and over 16 kJ/mol the adsorption type can be explained by a stronger chemical adsorption than ion exchange [31,22]. The values of E are found to be below 8 kJ/mol (Table 1) which corresponding to physical adsorption [32,33].

3.4.2. Error functions

Due to the inherent bias resulting from linearization, alternative isotherm parameter sets were determined by non-linear regression. This shows a mathematical method for determining isotherm parameters using the original form of the isotherm equation. In the single component isotherm studies, the optimization procedure requires an error function to be defined in order to be able to evaluate the fit of the isotherm to the experimental equilibrium data [34]. The choice of error function can affect the parameters derived-error functions based primarily on absolute deviation bias the fit toward high concentration data and this weighting increases when the square of deviation is used to penalize extreme errors. This bias can be offset partly by dividing the deviation by the measured value in order to emphasize the significance of fractional deviation.

In this study, five different error functions were examined and in each case the isotherm parameters were determined by minimizing the respective error function across the concentration range studied using the Solver add-in with Microsoft Excel. The error functions studied were detailed in the following sections.

The average percentage errors (APE) calculated according to Eq. (9) indicated the fit of between the experimental and predicated values of adsorption capacity used the plotting isotherm curves [35].

$$APE(\%) = \frac{100}{N} \times \sum_{i=1}^{N} \left| \frac{q_{e,isotherm} - q_{e,exp}}{q_{e,isotherm}} \right|_i \tag{9}$$

where $q_{e,isotherm}$ and q_{exp} are the values of q_e (mg/g) calculated by isotherm model and experimental equilibrium measurement, respectively.

The chi-square test statistic is basically the sum of the squares of the differences between the experimental data and data obtained by calculating from models, with each squared difference divided by the corresponding data obtained from by calculating from the models.

$$x^2 = \sum_{i=1}^{N} \frac{(q_{e,isotherm} - q_{e,exp})^2}{q_{e,isotherm}} \quad (10)$$

If the data from the model are similar to the experimental data, χ^2 will be a small number, while if they differ; χ^2 will be a bigger number. Therefore, it is necessary also to analyze the data set using the non-linear chi-square test to confirm the best-fit isotherm for the sorption system [36].

Marquardt's percent standard deviation (*MPSD*) error function was used previously by a number of researchers [37]. It is similar in some respects to a geometric mean error distribution modified according to the number of degrees of freedom of the system.

$$MPSD = 100 \times \sqrt{\frac{1}{N-P}\sum_{i=1}^{N} \frac{(q_{e,isotherm} - q_{e,exp})_i^2}{q_{e,isotherm}}} \quad (11)$$

The root mean square errors (*RMS*) are given as the following equation [35]:

$$RMS = 100 \times \sqrt{\frac{1}{N}\sum_{i=1}^{N} \left(1 - \frac{q_{e,exp}}{q_{e,isotherm}}\right)^2} \quad (12)$$

The average relative error (ARE) is an error function attempts to minimize the fractional error distribution across the entire concentration range [35]:

$$ARE = \frac{100}{P} \times \sum_{i=1}^{P} \left| \frac{q_{e,isotherm} - q_{e,exp}}{q_{e,isotherm}} \right| \quad (13)$$

The data obtained from different error functions are summarized in Table 2.

By comparing the values of different error functions, it was found that Freundlich isotherm model best fits the Ni^{2+} adsorption onto RD, DACI and DACII, respectively. The model shows high correlation coefficients and low% error value. Meanwhile, Fig. 4(a–c) shows plots comparing different isotherm equations with experimental data for RD, DACI and DACII, respectively. The figure shows an excellent fit of Freundlich model with experimental data for the adsorption of Ni^{2+} onto RD, DACI and DACII, while Langmuir isotherm model shows the lowest fit onto different adsorbents which confirms the results obtained by error analysis.

Table 2 The best-fit isotherm models to the experimental equilibrium data by several different errors functions.

Isotherm model	*APE%*	X^2	*MPSD*	*RMS*	*ARE*
	RD				
Frundlich	0.005	0.000	0.015	0.013	0.005
Langmuir	2.119	0.378	6.633	5.606	2.119
Tembkin	0.012	0.000	0.037	0.031	0.012
D–R	1.567	0.207	4.905	4.145	1.567
	DACI				
Frundlich	0.013	0.000	0.040	0.034	0.013
Langmuir	7.375	4.308	23.087	19.512	7.375
Tembkin	0.016	0.000	0.051	0.043	0.016
D–R	0.277	0.006	0.868	0.733	0.277
	DACII				
Frundlich	0.015	0.000	0.047	0.039	0.015
Langmuir	78.003	328.846	244.187	206.376	78.003
Tembkin	0.008	0.000	0.024	0.020	0.008
D–R	0.235	0.003	0.735	0.621	0.235

The comparison of Ni^{+2} adsorption capacities (Q_m) by various adsorbents is summarized in Table 3. The activated carbon used in this research showed higher adsorption capacity compared with some other activated carbon. Thus the utilization of doum-palm seed for the preparation of activated carbon for Ni^{+2} removal from aqueous solutions shows promising results.

3.5. Adsorption kinetics

The adsorption kinetics is one of the most important data in order to understand the mechanism of the adsorption and to assess the performance of the adsorbents. Different kinetic models including pseudo-first-order, pseudo-second-order and Elovich model were applied for the experimental data to predict the adsorption kinetics of nickel onto RD, DACI, and DACII.

3.5.1. The pseudo-first-order equation

The Lagergren's rate equation [53] is one of the most widely used rate equation to describe the adsorption of an adsorbate from the liquid phase. The linear form of pseudo-first-order equation is given as:

$$\log(q_e - q_t) = \log q_e - \frac{k_1}{2.303} t \quad (14)$$

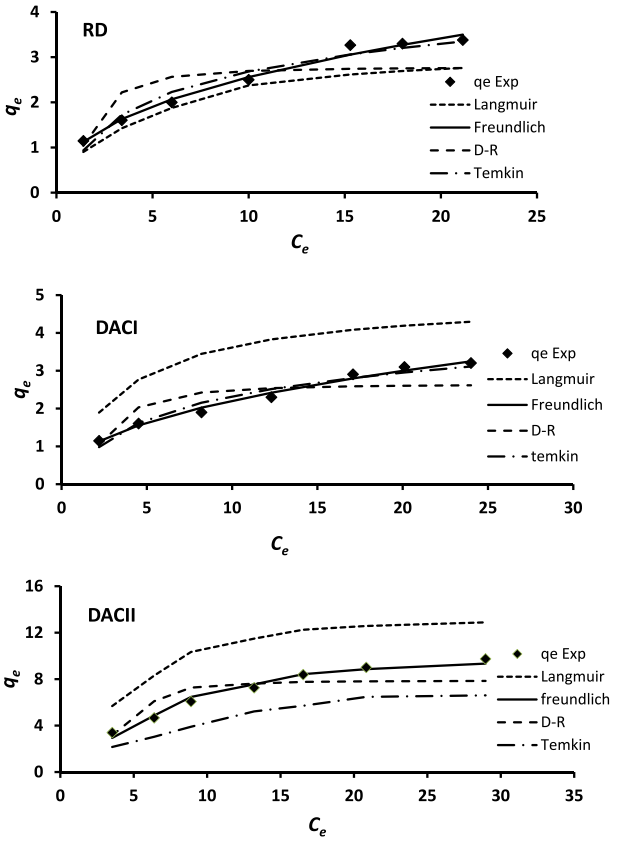

Figure 4 Equilibrium isotherms for the removal of Ni^{2+} ions on RD, DACI and DACII.

Table 3 Adsorption capacities of different adsorbents for nickel removal from aqueous solutions.

Adsorbent	Adsorption capacity (mg/g)	References
Chabazite	4.5	[38]
Clinoptilolite	0.9	[38]
Fly ash	0.03	[39]
Sheep manure waste	7.2	[40]
Banana peel	6.8	[41]
Hazelnut shell	10.1	[42]
Baker's yeast	11.4	[43]
Waste of tea factory	18.42	[44]
Alternanthera Philoxeroides biomass	9.73	[45]
Cone biomass of *Thuja orientalis*	12.42	[46]
Protonated rice bran	46.51	[47]
Rice husk	8.86	[13]
Natural iron oxide-coated sand	1	[48]
Calcined Bofe bentonite clay	3.893	[17]
Punica granatum peel waste	52.2	[49]
Aspergillus niger	28.1	[50]
Nano-hydroxyapatite	46.17	[51]
Nano-hydroxyapatite	40.00	[52]
RD	3.24	Present study
DACI	4.93	Present study
DACII	13.51	Present study

Table 4 Kinetic rate constants related to the sorption of Ni^{2+} onto RD, DACI and DACII.

Kinetics model	RD	DACI	DACII
Pseudo first order			
k_1 (l/min)	0.02	0.025	0.027
r^2	0.87	0.868	0.769
Pseudo second order			
k_2 (g/mg min)	0.04	0.08	0.05
r^2	0.992	0.996	0.985
Elovich equation			
α	5.1	91.21	1.65
β	3.48	6.17	4.42
r^2	0.946	0.841	0.915
Intraparticle diffusion			
K_{dif} (mg/(g $min^{1/2}$))	0.091	0.051	0.072
C (mg/g)	1.226	1.25	0.762
r^2	0.962	0.86	0.938

where q_t (mg/g) is the amount of nickel ions adsorbed at time t and k_1 (min^{-1}) is the rate constant of the pseudo-first-order adsorption model. The experimental results of the first order rate constants are presented in Table 4. The adsorption data have a poor regression coefficient (Table 4), which suggests that the adsorption of Ni^{2+} on activated carbon does not follow entirely the pseudo-first order adsorption kinetics.

3.5.2. The pseudo-second-order rate equation

The linear form of pseudo-second-order model is given by equation [54]:

$$\frac{t}{q_t} = \frac{1}{k_2 q_e^2} + \frac{t}{q_e} \tag{15}$$

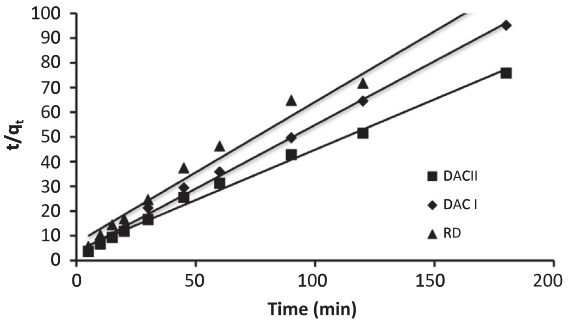

Figure 5 Pseudo-second order sorption kinetics of nickel ions onto RD, DACI and DACII.

where k_2 (g/(mg min)) is the rate constant of the pseudo-second order kinetic model. The relationship shows a good compliance with the pseudo second-order equation (Fig. 5). The correlation coefficient for the linear plot, r^2, suggests a strong relationship between the parameters and also explains that the process of adsorption follows pseudo-second-order kinetics (Table 4).

3.5.3. Elovich model

The Elovich model is employed to describe chemisorption and is given by the equation [55]:

$$q_t = \frac{1}{\beta}\ln(\alpha\beta) + \frac{1}{\beta}\ln(t) \tag{16}$$

where α is the initial sorption rate (mg/(g min)) and β is the desorption constant (g/mg). The plot q_t versus ln t having slope $1/\beta$ and intercept $[(1/\beta)\ln(\alpha\beta)]$. The values of α and β are given in Table 4 with a correlation coefficient ranging from 0.841 to 0.946.

In the view of these results, second order kinetic model provided a good correlation for the adsorption of Ni^{2+} ions onto RD, DACI, and DACII, in contrast to the pseudo-first-order and Elovich models.

3.6. Adsorption mechanism

Diffusion models were also employed to describe the nickel adsorption process. Three main steps are involved in the solid–liquid sorption process between the metal ions and the adsorbent [56]; (a) the metal ions are transferred from the bulk solution to the external surface of the adsorbent. This is known as film diffusion, (b) the metal ions are transferred within the pores of the adsorbent. This is known as intraparticle diffusion, occurring either as pore diffusion or as a solid surface diffusion mechanism, (c) the active sites on the surface of the adsorbent capture the metal ions.

The intraparticle diffusion model is given by the following equation [57]:

$$q_t = K_{dif} t^1/2 + C \tag{17}$$

where K_{dif} is the intra-particle diffusion rate constant (mg/(g min)), and C is a constant that gives an idea about the boundary layer thickness (mg/g).

The intraparticle diffusion plots of the experimental results, q_t versus $t^{1/2}$ for different adsorbent are shown in Fig. 6. The values of K_{dif} and correlation coefficients (r^2) obtained from

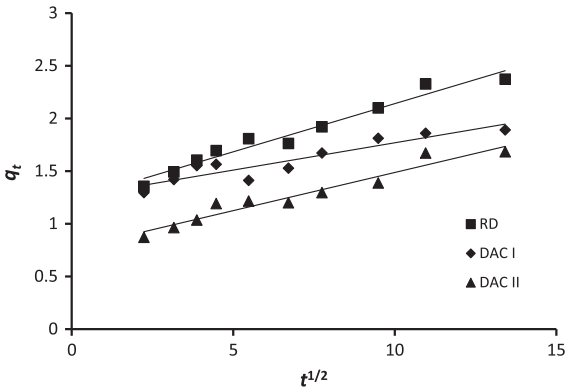

Figure 6 Intra-particle diffusion plots for the removal of nickel ions onto RD, DACI and DACII.

Table 5 Diffusion coefficients for Ni^{2+} sorption onto various adsorbents.

Type of adsorbent	Diffusion parameters	
	Film diffusion D_f (m^2/s)	Particle diffusion Dp (m^2/s)
RD	3.0447×10^{-07}	2.754×10^{-07}
DACI	4.1932×10^{-07}	3.765×10^{-07}
DACII	5.9076×10^{-07}	4.098×10^{-07}

intraparticle diffusion plots are given in Table 4. The values of C obtained from intraparticle diffusion model indicate that intraparticle diffusion may not be the controlling factor in determining the kinetics of the process and film diffusion controls the initial rate of the adsorption, it also indicates the thickness of the boundary layer.

To identify weather external mass transfer (boundary layer diffusion) or intraparticle diffusion, or both combined is suitable to the Ni^{2+} biosorption onto RD, DACI, and DACII, the two diffusion coefficients D_f and D_p were calculated using the film and intraparticle diffusion models presented by the following equations respectively [58];

$$\ln\left(1 - \frac{q_t}{Q_m}\right) = -2k_p t \tag{18}$$

$$\ln\left(1 - \frac{q_t}{Q_m}\right) = -k_f t \tag{19}$$

where q_t is the Ni^{2+} amount removed at time t (mg/g); Q_m is the maximum amount of Ni^{2+} removed (mg/g); k_p and k_f are the rate constants which values are as (D_p π^2 r^{-2}) and (D_f C_e C_b^{-1} h^{-1}) respectively; r is the radius of adsorbent (cm); t is the time (s); h is the thickness of film, given as 10^{-4} cm for poorly stirred solution (cm); C_e and C_b are the concentrations of Ni^{2+} in the solution and in the biosorbent, respectively. The values of diffusion coefficients given in Table 5 indicate that for all adsorbents, the Ni^{2+} biosorption is governed by film diffusion process in the initial stages of adsorption then intraparticle diffusion.

3.7. Characterization of the biosorbent

3.7.1. Morphology analysis

In order to get an idea of the microscopic structure of the biosorbent surface and to estimate the biosorption mechanisms,

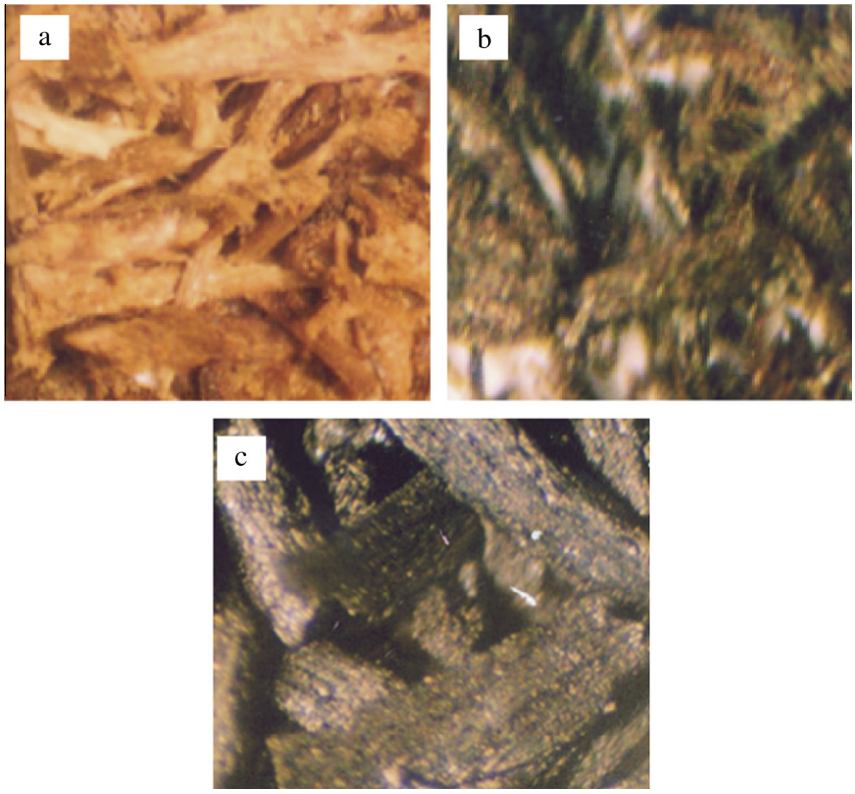

Figure 7 Micrograph photo of the surface of (a) RD; (b) DACI and (c) DACII.

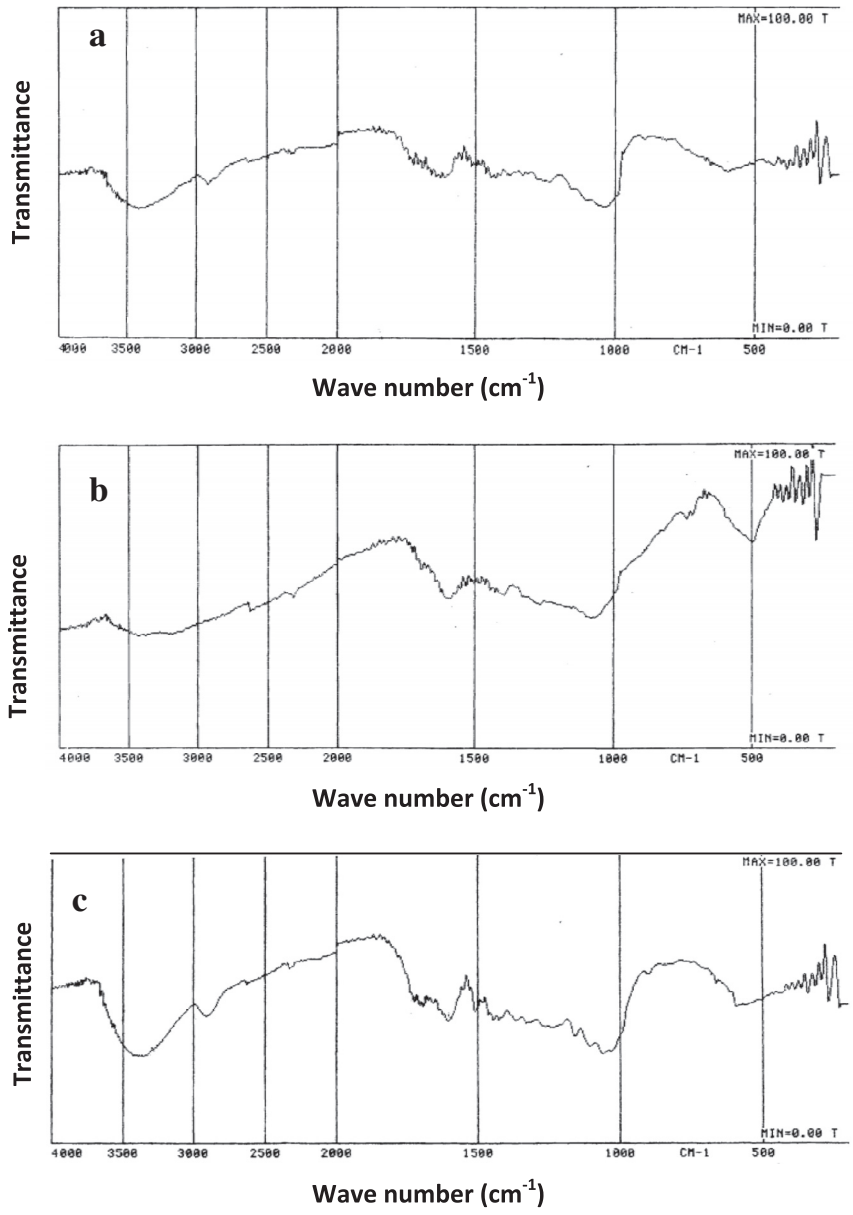

Figure 8 FTIR spectra of (a) RD; (b) DACI and (c) DACII adsorbents.

the surface of RD, DACI, and DACII was determined by magnification. Fig. 7(a–c) shows a photo of RD, DACI, and DACII, respectively, indicating that all adsorbent surfaces are very rough with the presence of cracks and cavities which very likely play a major role in the biosorption and intraparticle diffusion.

3.8. FTIR analysis

FTIR spectral analysis was done before and after modification of adsorbents RD, DACI and DACII to find out the involvement of functional groups in different adsorbents (Fig. 8(a–c)). A broad band between 3100 and 3700 cm^{-1} indicates the presence of both free and hydrogen bonded OH groups on the adsorbent surface. This stretching is due to both the silanol group (Si OH) and adsorbed water on the surface of adsorbent (Fig. 8a). The bands appearing in spectra of RD at 3452 cm^{-1} indicate hydrogen bonding. The peak at 1039 cm^{-1} may be assigned to vibration of the hydroxyl group combined with Mn atoms [59]. The peaks at 1100–1200 cm^{-1} could indicate the presence of alcohols and phenolic groups in both carbonized samples DACI and DACII (Fig. 8(b and c)) samples. The peak at 1025 cm^{-1} indicative –CO,–C–O, –COO– indicates of existing groups involved in sorption mechanisms. In addition to the P–O stretching modes, a deformation mode has been detected, at 1250 for DACII due to the treatment of H_3PO_4 acid before carbonization (Fig. 8c).

4. Conclusions

Doum-palm seed coat (RD) and two activated carbons had been prepared from it (DACI and DACII) were used as

adsorbents for Ni^{2+} ions removal. The process parameters were optimized; initial Ni^{2+} ion concentration and dose of adsorbent were found to have significant effects on Ni^{2+} adsorption, at optimum initial pH of the solution. DACII has been found to have the maximum adsorption capacity. Under optimum conditions, 1 g of DACII can remove around 13.51 mg of nickel ions from aqueous solution. The adsorption process follows Freundlish isotherm model for all adsorbents. The results were analyzed by the modeling equations which indicated that the external transport is favored by the initial time while the internal transport is more favored after long time. The use of DACII in the treatment of wastewater for the removal of Ni^{2+} ions could be a low cost technology and a promising recycling strategy of corps wastes and nutrients in wastewater.

References

[1] B. Qin, H. Luo, G. Liu, R. Zhang, S. Chen, Y. Hou, Y. Luo, Nickel ion removal from wastewater using the microbial electrolysis cell, Bioresour. Technol. 121 (2012) 458–461.

[2] A. Bhatnagar, A.K. Minocha, Biosorption optimization of nickel removal from water using *Punica granatum* peel waste, Colloid Surface B. 76 (2010) 544–548.

[3] M.G.A. Vieira, A.F.A. Neto, M.L. Gimenes, M.G.C. da Silva, Sorption kinetics and equilibrium for the removal of nickel ions from aqueous phase on calcined Bofe bentonite clay, J. Hazard. Mater. 177 (2010) 362–371.

[4] N. Boujelben, J. Bouzid, Z. Elouear, Adsorption of nickel and copper onto natural iron oxide-coated sand from aqueous solutions: study in single and binary systems, J. Hazard. Mater. 163 (1) (2009) 376–382.

[5] E. Katsou, S. Malamis, K.J. Haralambous, M. Loizidou, Use of ultrafiltration membranes and aluminosilicate minerals for nickel removal from industrial wastewater, J. Membr. Sci. 360 (2010) 234–249.

[6] US EPA, Guidelines for Water Reuse, EPA/625/R-04/108, U.S. Agency for Inter. Development, Washington, DC, USA, 2004.

[7] N. Ghasemi, M. Ghasemi, S. Mashhadi, M.H. Tarraf, International Congress on Informatics, Environment, Energy and Applications-IEEA 2012 IPCSIT, vol. 38, IACSIT Press, Singapore, 2012.

[8] Z.Z. Chowdhury, S.M. Zain, R. Atta Khan, A.A. Ahmed, Equilibrium kinetics and isotherm studies of Cu (II) adsorption from waste water onto alkali activated oil palm ash, Am. J. Appl. Sci. 8 (2011) 230–237.

[9] O.A. Eldahshan, N.A. Ayoub, A.B. Singab, M.M. Al-Azizi, Potential antioxidant phenolic metabolites from doum palm leaves, Afr. J. Pharm. Pharmacol. 3 (4) (2009) 158–164.

[10] N.K. Amin, O. Abdelwahab, Comparative Study of Heavy Metal removal by *Hyphaene thebaica* adsorbents, Blue Biotechnol. J. 1 (4) (2012) 581–597.

[11] K.M. Doke, E.M. Khan, Equilibrium, kinetic and diffusion mechanism of Cr (VI) adsorption onto activated carbon derived from wood apple shell, Arab. J. Chem. (2012), doi: http://dx.doi.org/10.1016/j.arabjc.2012.07.031.

[12] M. Jain, V.K. Garga, K. Kadirvelu, Chromium (VI) removal from aqueous system using Helianthus annuus (sunflower) stem waste, J. Hazard. Mater. 162 (2009) 365–372.

[13] M. Bansal, D. Singh, V.K. Garg, P. Rose, Use of agricultural waste for the removal of nickel ions from aqueous solutions: equilibrium and kinetics studies, Int. J. Civil Environ. Eng. 1 (2) (2009) 108–114.

[14] K.C. Sekher, S. Subramanian, J.M. Modak, K.A. Natarajan, Removal of metal ions using an industrial biomass with reference to environmental control, Int. J. Miner. Process. 53 (1998) 107–120.

[15] E. Malkoc, Ni (II) removal from aqueous solutions using cone biomass of Thuja orientalis, J. Hazard. Mater. 137 (2) (2006) 899–908.

[16] R. Gupta, H. Mohapatra, Microbial biomass: an economical alternative for removal of heavy metals from waste water, Indian J. Exp. Biol. 41 (2003) 945–966.

[17] M.G.A. Vieira, A.F. Almeida Neto, M.L. Gimenes, M.G.C. da Silva, Sorption kinetics and equilibrium for the removal of nickel ions from aqueous phase on calcined Bofe bentonite clay, J. Hazard. Mater. 177 (2010) 362–371.

[18] S.S. Gupta, K.G. Bhattacharyya, Immobilization of Pb(II), Cd(II) and Ni(II) ions on kaolinite and montmorillonite surfaces from aqueous medium, J. Environ. Manage. 87 (1) (2008) 46–58.

[19] S. Al-Asheh, F. Banat, L. Abu-Aitah, Adsorption of phenol using different types of activated bentonites, Sep. Purif. Technol. 33 (2003) 1–10.

[20] S. Yapar, V. Özbudak, A. Dias, A. Lopes, Effect of adsorbent concentration to the adsorption of phenol on hexadecyl trimethyl ammonium-bentonite, J. Hazard. Mater. B121 (2005) 135–139.

[21] A. Shukla, Y.-H. Zhang, P. Dubey, J.L. Margrave, S.S. Shukla, The role of sawdust in the removal of unwanted materials from water, J. Hazard. Mater. 95 (2002) 137–152.

[22] I. Mobasherpour, E. Salahi, M. Pazouki, Removal of nickel (II) from aqueous solutions by using nano-crystalline calcium hydroxyapatite, J. Saudi Chem. Soc. 15 (2011) 105–112.

[23] I. Langmuir, The adsorption of gases on plane surfaces of glass, mica and platinum, J. Am. Chem. Soc. 40 (1918) 1361–1403.

[24] K.R. Hall, L.C. Eagleton, A. Acrivos, T. Vermeule, Pore- and solid-diffusion kinetics in fixed-bed adsorption under constant-pattern conditions, Ind. Eng. Chem. Fund. 5 (1966) 212–223.

[25] H.M. Freundlich, Over the adsorption in solution, Z. Phys. Chem. 57 (1906) 385–470.

[26] G. Crini, H.N. Peindy, Adsorption of CI Basic Blue on cyclodextrin-based material containing carboxylic groups, Dyes Pigme. 70 (2006) 204–211.

[27] C. Aharoni, M. Ungarish, Kinetics of activated chemisorptions. Part 2. Theoretical models, J. Chem. SocFaraday Trans. 73 (1977) 456–464.

[28] D.H.K. Reddy, K. Seshaiah, A.V.R. Reyddy, M.M. Rao, M.C. Wang, Biosorption of Pb+2 from aqueous solutions by Moringa oleifera bark: equilibrium and kinetic studies, J. Hazard. Mater. 174 (2010) 831–838.

[29] M.M. Dubinin, The potential theory of adsorption of gases and vapors for adsorbents with energetically non-uniform surface, Chem. Rev. 60 (1960) 235–266.

[30] S.M. Hasany, M.H. Chaudhary, Sorption potential of Hare River sand for the removal of antimony from acidic aqueous solution, Appl. Radiat. Isot. (1996) 467–471.

[31] C.C. Wang, L.C. Juang, C.K. Lee, T.C. Hsua, J.F. Leeb, H.P. Chaob, Effects of exchanged surfactant cations on the pore structure and adsorption characteristics of montmorillonite, J. Colloid Interface Sci. 280 (2004) 27–35.

[32] P. Djomgoue, M. Siewe, E. Djoufac, P. Kenfack, D. Njopwouo, Surface modification of Cameroonian magnetite rich clay with Eriochrome Black T. Application for adsorption of nickel in aqueous solution, Appl. Surf. Sci. 258 (2012) 7470–7479.

[33] S. Elsherbiny, T.A. Fayed, Adsorption study of dimethyla minostyryl benzazoles onto Na-montmorillonite, J. Phys. Chem. Solids 71 (2010) 952–957.

[34] L.S. Chan, W.H. Cheung, S.J. Allen, G. McKay, Error analysis of a dsorption isotherm models for acid dyes onto bamboo derived activated carbon, Chin. J. Chem. Eng. 20 (3) (2012) 535–542.

[35] J.C.Y. Ng, W.H. Cheung, G. McKay, Equilibrium studies of the sorption of Cu (II) ions onto chitosan, J. Colloid Interf Sci. 255 (2002) 64–74.

[36] S. Meenakshi, N. Viswanathan, Identification of selective ion-exchange resin for fluoride sorption, J Colloid Interf Sci. 308 (2007) 438–450.
[37] A. Seidel, D. Gelbin, On applying the ideal adsorbed solution theory to multicomponent adsorption equilibria of dissolved organic components on activated carbon, Chem. Eng. Sci. 43 (1988) 79–89.
[38] S.K. Ouki, M. Kavannagh, Treatment of metals-contaminated wastewaters by use of natural zeolites, Water Sci. Technol. 39 (1999) 115–122.
[39] M. Rao, A.V. Parwate, A.G. Bhole, Removal of Cr^{6+} and Ni^{2+} from aqueous solution using bagasse and fly ash, Waste Manage. 22 (2002) 821–830.
[40] F. Abu Al-Rub, M. Kandah, N. Aldabaibeh, Nickel removal from aqueous solutions using sheep manure wastes, Eng. Life Sci. 2 (2002) 111–116.
[41] G. Annadurai, R.S. Juang, D.J. Lee, Adsorption of heavy metals from water using banana and orange peels, Water Sci. Technol. 47 (1) (2002) 185–190.
[42] E. Demirbaş, M. Kobya, S. Öncel, S. Şencan, Removal of Ni(II) from aqueous solution by adsorption onto hazelnut shell activated carbon: equilibrium studies, Bioresour. Technol. 84 (3) (2002) 291–293.
[43] V. Patmavathy, P. Vasudevan, S.C. Dhingra, Adsorption of nickel(II) ions on Baker's yeast, Process Biochem. 38 (2003) 1389–1395.
[44] F.P. Padilha, F.P. de França, A.C.A. da Costa, The use of waste biomass of Sargassum sp. for the biosorption of copper from simulated semiconductor effluents, Bioresour. Technol. 96 (2005) 1511–1517.
[45] X.S. Wang, Y. Qin, Removal of Ni(II), Zn(II) and Cr(VI) from aqueous solution by Alternanthera philoxeroides biomass, J. Hazard. Mater. B 138 (2006) 582–588.
[46] E. Malkoc, Ni(II) removal from aqueous solutions using cone biomass of Thuja orientalis, J. Hazard. Mater. B 137 (2006) 899–908.
[47] M.N. Zafar, R. Nadeem, M.A. Hanif, Biosorption of nickel from protonated rice bran, J. Hazard Mater. 143 (2007) 478–485.
[48] N. Boujelben, J. Bouzid, Z. Elouear, Adsorption of nickel and copper onto natural iron oxide-coated sand from aqueous solutions: Study in single and binary systems, J. Hazard Mater. 163 (2009) 376–382.
[49] A. Bhatnagar, A.K. Minocha, Biosorption optimization of nickel removal from water using Punica granatum peel waste, Colloid Surfaces B. 76 (2010) 544–548.
[50] K. Munir, M. Yusuf, A. Hameed, F.Y. Hafeez, R. Faryal, Isotherm studies for determination of removal capacity of BI-metal (Ni and Cr) ions by *Aspergillus niger*, Pakistan J. Bot. 42 (1) (2010) 593–604.
[51] I. Mobasherpour, E. Salahi, M. Pazouki, Removal of nickel (II) from aqueous solutions by using nano-crystalline calcium hydroxyapatite, J. Saudi Chem. Soc. 15 (2011) 105–112.
[52] I. Mobasherpour, E. Salahi, M. Pazouki, Comparative of the removal of Pb2+, Cd^{2+} and Ni^{2+} by nano crystallite hydroxyapatite from aqueous solutions: adsorption isotherm study, Arab J. Chem. 5 (4) (2012) 439–446.
[53] S. Lagergren, Zur theorie der sogenannten adsorption geloster stoffe 591, Kungliga Svenska Vetenskapsakademiens, Handlingar 24 (4) (1898) 1–39.
[54] Y.S. Ho, G. McKay, Kinetic models for the sorption of dye from aqueous solution by wood, J. Environ. Sci. Health Part B: Process Saf. Environ. Protect. 76 (1998) 183–191.
[55] X.S. Wang, Z.Z. Li, S.R. Tao, Removal of chromium (VI) from aqueous solution using walnut hull, J. Environ. Manage. 90 (2009) 721–729.
[56] M.H. Kalavathy, T. Karthikeyan, S. Rajgopal, L.R. Miranda, Kinetic and isotherm studies of Cu(II) adsorption onto H3PO4 – activated rubber wood sawdust, J. Colloid Interf. Sci. 292 (2005) 354–362.
[57] W.J. Weber Jr., J.C. Morriss, Kinetics of adsorption on carbon from solution, J. Sanitary Eng. Div. Am. Soc. Civ. Eng. 89 (1963) 31–60.
[58] M.A. Wahab, H. Boubakri, S. Jellali, N. Jedidi, Characterization of ammonium retention processes onto Cactus leaves fibers using FTIR, EDX and SEM analysis, J. Hazard. Mater. 241–242 (2012) 101–109.
[59] G.S. Zhang, J.H. Qu, H.J. Liu, R.P. Liu, G.T. Li, Removal mechanism of As(III) by a novel Fe-Mn binary oxide adsorbent: oxidation and sorption, Environ. Sci. Technol. 41 (2007) 4613–4619.